Raman microspectroscopy of intracellular cholesterol crystals in cultured bovine coronary artery endothelial cells

Sharon R. Hawi,* Kasem Nithipatikom,[1,]* Eric R. Wohlfeil,[†] Fran Adar,[§] and William B. Campbell*

Departments of Pharmacology and Toxicology* and Anesthesiology,[†] Medical College of Wisconsin, 8701 Watertown Plank Road, Milwaukee, WI 53226, and Instruments, S.A., Inc.,[§] 3880 Park Avenue, Edison, NJ 08820

Abstract Raman microspectroscopy is presented as a promising technique for the in situ characterization of intracellular cholesterol crystals. Crystal characterization is the first step in investigating the effects of various stimuli on their formation and in determining their role in the development of atherosclerosis. Treatment of cultured bovine coronary artery endothelial cells with 22-hydroxycholesterol (220HC) stimulated the production of intracellular crystals, a phenomenon that did not occur in the absence of viable cells. These crystals were identified as a combination of the 220HC starting material and cholesterol. The best fit to the average Raman spectrum of the microscopic crystals was achieved with a combination of 70% Raman contribution from 220HC and 30% from cholesterol. GC/MS analysis of the crystals confirmed the presence of both compounds. These results demonstrate the potential of Raman microspectroscopy as a powerful tool in lipid research, particularly for the in situ characterization of intracellular crystals.—**Hawi, S. R., K. Nithipatikom, E. R. Wohlfeil, F. Adar, and W. B. Campbell.** Raman microspectroscopy of intracellular cholesterol crystals in cultured bovine coronary artery endothelial cells. *J. Lipid Res.* 1997. **38:** 1591–1597.

Supplementary key words cholesterol • 22-hydroxycholesterol • oxysterol • confocal Raman microspectroscopy • intracellular crystals • atherosclerosis

The formation of atherosclerotic lesions is believed to be initiated by injury to the endothelium of blood vessels (1). The progression of these lesions relies, in part, upon cellular uptake of lipid compounds, such as cholesterol and its derivatives, with a key intermediate step being the precipitation of excess cholesterol in the form of crystals (2). High concentrations of the oxygenated cholesterol derivatives, the oxysterols, have also been found in human atherosclerotic lesions (3, 4).

We are currently investigating the effects of oxysterols on vascular endothelial cells to determine their role in atherogenesis. In particular, we have measured the production of eicosanoids by bovine coronary artery endothelial cells treated with various hydroxycholesterols (5). Interestingly, we found that treatment with 22(S)-hydroxycholesterol stimulated the production of intracellular crystals. Crystal formation in a cell culture system may serve as a model for the arterial crystal deposition that is associated with atherosclerosis, provided that the crystals can be characterized.

In a recent report of intracellular crystal formation in a culture of cholesteryl ester-loaded macrophage foam cells, density and melting point measurements were used to characterize the crystals and identify them as cholesterol monohydrate (6). These identification techniques required isolation and physical alteration of the microscopic crystals.

Raman microspectroscopy, on the other hand, is a non-invasive, non-destructive identification technique that relies on inelastic scattering of light by a sample. It is suitable for aqueous environments and can provide structural information in situ, making it an attractive alternative for the characterization of intracellular crystals. Technological improvements in sensitivity and spatial resolution have drawn attention to Raman microspectroscopy as a useful tool in biomedical research (7, 8), particularly in the identification of foreign material in biological samples (9–13). Raman spectroscopy has been applied to cholesterol-related research in a num-

Abbreviations: 220HC, 22-hydroxycholesterol; TMS, bis(trimethylsilyl)-trifluoroacetamide; GC/MS, gas chromatography–mass spectrometry; PCI, positive chemical ionization.

[1]To whom correspondence should be addressed.

ber of different fields. For example, it has been used for the differentiation of cholesterol and bilirubin components in gallstones (14), for the measurement of eye lens transparency and its relation to cataract formation (15), and the analysis of cholesteryl ester mixtures as a model of the arterial lumina (16). In this work, we demonstrate the potential of Raman microspectroscopy in lipid research by characterizing the microscopic crystals that formed within cultured bovine coronary artery endothelial cells upon treatment with 22-hydroxycholesterol.

MATERIALS AND METHODS

Materials

Cholesterol and 22(S)-hydroxycholesterol (22OHC) were purchased from Sigma Chemical Co. (St. Louis, MO) and recrystallized from HPLC grade acetone (Mallinckrodt, Paris, KY). Cholesteryl oleate was obtained from U.S. Biochemical Corporation (Cleveland, OH) and used as received. Fetal bovine serum was obtained from JRH Biosciences (Lenexa, KS), RPMI 1640 media and L-glutamine were obtained from Life Technologies (Gaithersburg, MD), and all other culture materials were purchased from Sigma. Quartz microscope slides were purchased from Thomas Scientific (Swedesboro, NJ).

Cell cultures and intracellular crystal formation

Endothelial cells were collected from bovine coronary arteries and cultured as previously described (17). Briefly, cells were collected from the lumen of bovine coronary arteries using 0.1% (w/v) collagenase in RPMI 1640 media. The cells were washed with 25 mM HEPES buffer, pH 7.4, containing 150 mM NaCl, 5 mM KCl, 1.8 mM $CaCl_2$, 1 mM $MgCl_2$, and 6 mM glucose. They were then plated into culture flasks and incubated at 37°C in an atmosphere of 5% CO_2 in air. The RPMI 1640 culture media contained 25 mM HEPES and was supplemented with 15% fetal bovine serum, 1% L-glutamine, 3 μL/mL gentamycin, 3 μL/mL nystatin, 1 μL/mL tylosin, and 1% antibiotic antimycotic solution. When cells were 80% confluent, a solution of 10 mg/mL 22OHC in ethanol was added to the feed media for a final 22OHC concentration of 10 μg/mL. Continuous exposure to the 22OHC, with daily replacement of the treated media, produced needle-like intracellular crystals after 1–2 days. Control samples of media alone and media with nonviable cells were treated with 22OHC and incubated in the same manner.

Raman microspectroscopy

For Raman microspectroscopic analysis, cells were grown on quartz microscope slides stored in glass petri dishes, following the procedure outlined above. Upon crystal formation, the phenol red-tinted RPMI medium was removed by washing the slides with HEPES buffer solution, pH 7.4. A small amount of buffer solution remained on the cells to avoid dehydration.

Raman spectra were recorded with an Explorer series confocal Raman microspectrometer (Instruments, S.A., Inc., Edison, NJ), equipped with a 12 mW helium-neon laser excitation source at 632.8 nm, an Olympus BH-2 microscope with an 80× (NA 0.75) objective, a holographic notch filter (Kaiser Optical Systems, Ann Arbor, MI) to reject Rayleigh scattered light, a single monochromator (ISA HR 460) with a 600 gr/mm grating to disperse the Raman scattered light with a spectral resolution of 6–7 cm^{-1}, and a thermo-electrically cooled 1024 × 256 pixel CCD detector. The focused laser beam gave a lateral resolution of 1 μm, and a 200 μm confocal aperture positioned in the back image plane of the microscope provided an axial resolution of better than 10 μm. Peak frequencies were calibrated with the silicon phonon line at 520 cm^{-1}.

Gas chromatography/mass spectrometry (GC/MS)

Crystals were collected from the cell culture media by combining the spent media from several days of 22OHC treatment and filtering it through a 0.2-μm nylon membrane (Alltech Associates, Inc., Deerfield, IL). The spent media typically contained free crystals released from cells, as well as crystals attached to cellular debris. After several cold water washes, the collected crystals were dissolved in anhydrous acetonitrile and derivatized with bis(trimethylsilyl)-trifluoroacetamide (TMS) (Supelco Inc., Bellefonte, PA) by incubating for 1 h at 37°C. The organic solvent was dried and the sample was redissolved in 50 μL acetonitrile. Cholesterol and 22OHC standards were also derivatized and prepared in the same manner.

The derivatized samples were injected into a 5890 Series II gas chromatograph/5989A MS Engine mass spectrometer (GC/MS) (Hewlett-Packard, Palo Alto, CA) using an autosampler. Separation was accomplished by a 30 m DB-5 capillary column of 0.25 mm i.d. and 0.25 μm film thickness (J&W Scientific, Folsom, CA). Detection was made in positive chemical ionization (PCI) mode using methane as the reagent gas and a source temperature of 250°C. The GC injection port temperature was 250°C, and the column temperature was increased from 100°C to 300°C at a rate of 20°C/min, and held at 300°C for 10 min.

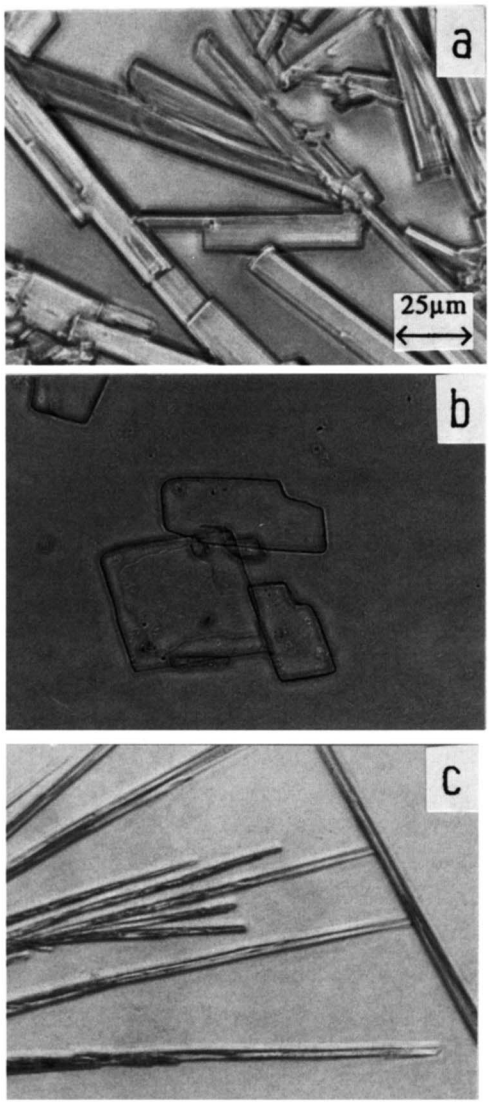

Fig. 1. Phase contrast light micrographs of a) anhydrous cholesterol needles, b) cholesterol monohydrate plates, and c) 22OHC needles. All frames were recorded at 400× magnification, as indicated by the scale bar in (a).

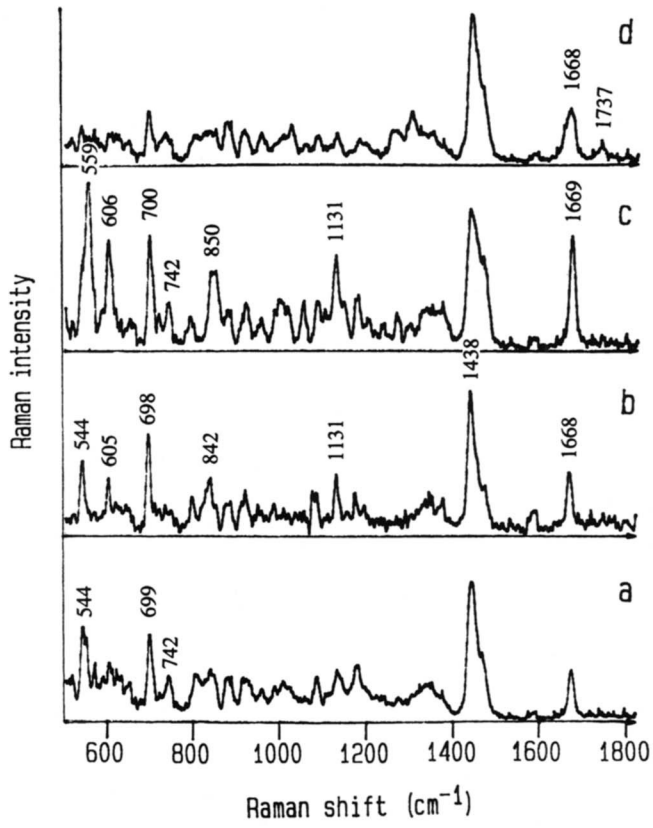

Fig. 2. Raman spectra of crystalline a) anhydrous cholesterol b) cholesterol monohydrate (in water), c) 22OHC, and d) cholesterol oleate in the 500–1800 cm^{-1} region, baseline-subtracted and normalized to the 1438 cm^{-1} band. All spectra represent 15-min acquisitions except that of cholesterol monohydrate (30 min).

RESULTS

Cholesterol and its derivatives

Recrystallization of cholesterol from anhydrous and aqueous acetone produced anhydrous cholesterol needles (**Fig. 1a**) and cholesterol monohydrate plates (Fig. 1b), respectively, in agreement with previous reports (18–20). Monohydrate crystals were stored in water to prevent dehydration. 22OHC also crystallized as needles from anhydrous acetone (Fig. 1c).

The Raman spectra of anhydrous cholesterol, cholesterol monohydrate, 22OHC, and cholesteryl oleate in the 500–1800 cm^{-1} region are compared in **Fig. 2.** The anhydrous (Fig. 2a) and hydrated (Fig. 2b) cholesterol spectra agree with previous reports (21). These spectra show that the various forms of cholesterol can be differentiated by their Raman characteristics. Although several bands, such as those near 700, 1438, and 1668 cm^{-1}, appear in all forms of cholesterol, their relative intensities often differ. In the oleate, for example, bands due to the cholesterol moiety are less pronounced, and vibrations of the attached hydrocarbon chain dominate the spectrum. A weak C═O stretch is also visible at 1737 cm^{-1}. The Raman spectrum of 22OHC is distinguished by its intense bands at 559, 606, and 1669 cm^{-1}. Even the anhydrous and monohydrated forms of cholesterol can be differentiated by their intensities at 742, 842, and 1131 cm^{-1}. The 742 cm^{-1} band appears stronger in the anhydrous form, while the 842 and 1131 cm^{-1} bands are more prominent in the monohydrate.

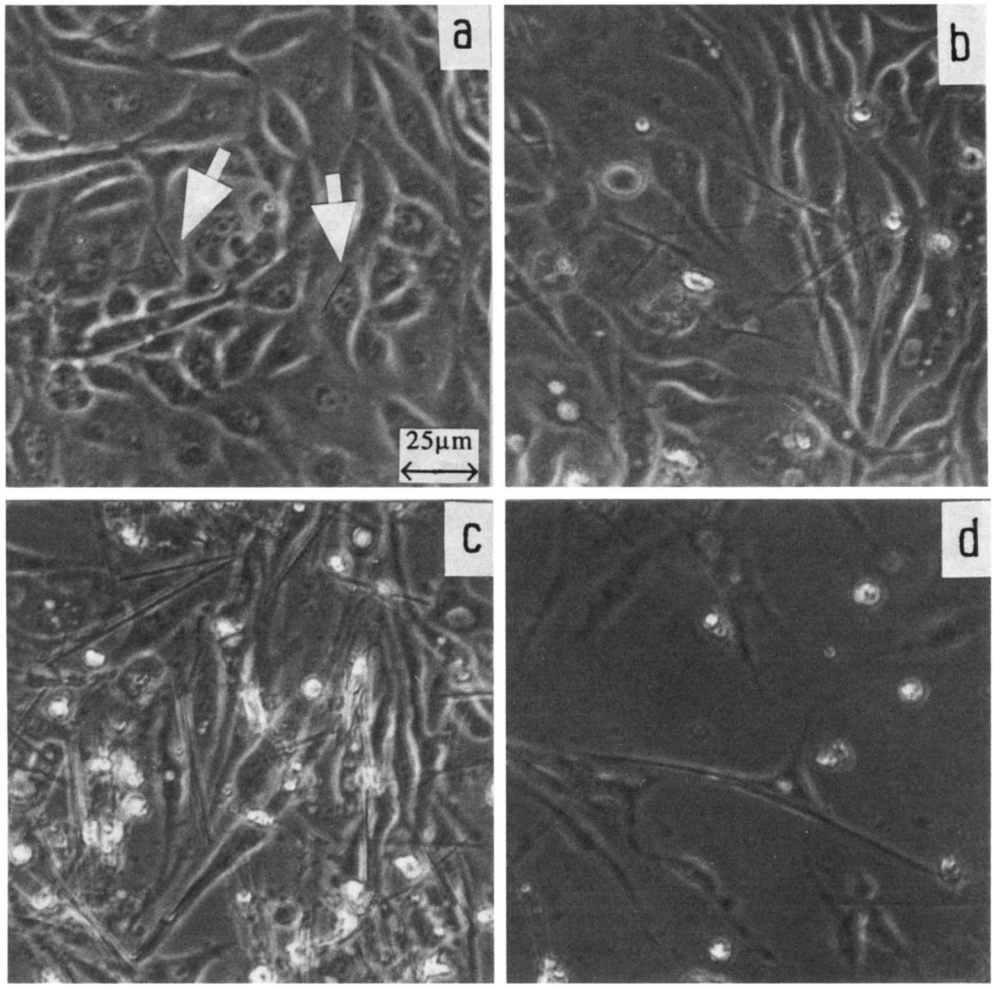

Fig. 3. Phase contrast light micrographs of endothelial cells after a) 1, b) 3, c) 5, and d) 6 days of 22OHC treatment. Initial crystal formation occurs within the cells, as indicated by arrows in frame (a). Several larger crystals are visible after 3 days, and by day 5 they are more numerous than the cells. After 6 days of treatment, very few cells remained adhered to the substrate, as in frame (d). Frame (d) also shows how the crystals tend to stretch the cell membrane during growth. All frames were recorded at 400× magnification, as indicated by the scale bar in (a).

Intracellular crystals

The formation and growth of intracellular crystals was recorded with phase-contrast photographs taken at 24-h intervals. **Figure 3** shows the progression from one day after the initial 22OHC treatment, where the crystals appear to originate within the endothelial cells, to days 3–5 of 22OHC treatment, where the crystals lengthen, often stretch the cell membrane, and appear more numerous, and finally to day 6 of 22OHC treatment, where the cells ultimately die and no longer adhere to the substrate. Crystals attached to cellular debris were then dispersed throughout the media. Vehicle (ethanol) control studies showed no significant change in cell appearance or viability. More importantly, control flasks of culture media alone and media with nonviable cells did not form crystals, indicating that crystal formation was dependent upon interaction with viable cells.

Raman microspectroscopy was performed on the intracellular crystals while the cells were attached to the substrate, typically 2–4 days after the initial 22OHC treatment. Control experiments using anhydrous cholesterol needles showed that crystal orientation within the field had no effect on the unpolarized Raman spectrum. Indeed, Raman spectra of the intracellular crystals at various orientations were identical, and the averaged spectrum is shown in **Fig 4a.** This spectrum does not match any of the individual cholesterol derivatives displayed in Fig. 2. However, a strong contribution

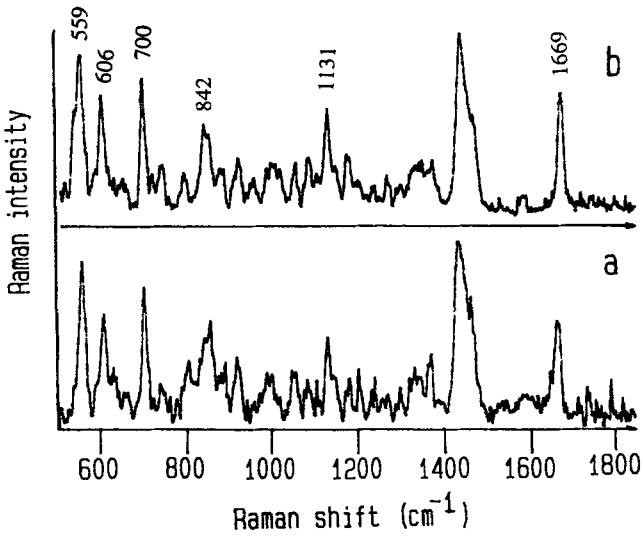

Fig. 4. Raman spectra of a) crystals that formed within endothelial cells, average of five crystals at various orientations, 30-min acquisitions, background-subtracted, and b) a combination of 70% Raman contribution from 22OHC (Fig. 2c) and 30% from cholesterol (Fig. 2b).

clearly arises from 22OHC, as evidenced by the 559 cm^{-1} band. The best fit to the observed crystal data was achieved with a spectrum consisting of 70% Raman contribution from 22OHC and 30% from cholesterol (Fig. 4b). Due to the small contribution from cholesterol and the similar Raman spectra of its anhydrous and monohydrated forms, both forms produced equally suitable fits.

The fact that both 22OHC and cholesterol contribute to the Raman spectrum of the intracellular crystals suggests that these two components have co-crystallized. To confirm these results, mixed crystals were prepared from 50/50 and 30/70 mixtures of cholesterol and 22OHC in acetone. The needle-like crystals that formed from these solutions were not completely homogeneous (i.e., the Raman spectra obtained from different crystals or at various positions on a single crystal were not always identical), but there was clear evidence of co-crystallization.

The chromatogram of the intracellular crystals and their corresponding PCI mass spectra are shown in **Fig. 5.** The retention times of peaks 1 (14.1 min) and 2 (14.9 min) of Fig. 5a matched those of pure cholesterol and 22OHC standards, respectively. The mass spectrum of peak 1 indicates that $(M-1)^+ = 457$ and $(M-CH_3)^+ = 443$, which correspond to cholesterol–TMS. The loss of (–OTMS) is indicated by the presence of ions at $m/z = 369$ and $m/z = 353$. The mass spectrum of peak 2 is identical to that of 22OHC–TMS, with $(M-1)^+ = 545$, $(M-CH_3)^+ = 531$, and a fragment from the 22-position to give $m/z = 173$. In this case, the loss of (–OTMS) is indicated by ions at $m/z = 455$ and $m/z = 441$.

DISCUSSION

The formation of intracellular crystals in cell culture systems can be used as a model for the study of the arterial crystal deposition that leads to atherosclerosis, provided that the intracellular crystals can be characterized. In this study, we have used Raman microspectroscopy for the non-invasive, non-destructive characterization of crystals that formed in cultured bovine coronary artery endothelial cells upon treatment with 22OHC. These crystals were identified as a combination of 22OHC and cholesterol. The best fit to the average Raman spectrum of the microscopic crystals was achieved with a combination of 70% Raman contribution from 22OHC and 30% from cholesterol.

An in situ quantitative analysis could not be performed because the Raman contribution of each component depends upon its molecular concentration as well as its inherent Raman scattering ability (Raman cross-section). An attempt to generate a standard curve of crystal composition versus observed Raman character was unsuccessful because these two components formed nonhomogeneous mixed crystals from solution. By comparison, the intracellular crystals were more uniform in composition, suggesting that they may form by a different, perhaps cell-regulated, mechanism.

External analysis of the intracellular crystals by GC/MS confirmed the presence of both cholesterol and 22OHC, but their relative concentrations could not be determined because the filtered sample consisted of crystals as well as cellular debris. This debris may have contained inherent cellular cholesterol, which would be indistinguishable from the crystalline cholesterol. Indeed, GC/MS analysis of crystal-free endothelial cells, prepared in the same manner as the treated cells, indicated the presence of some inherent cellular cholesterol (data not shown). The relative contributions of crystalline and cellular cholesterol to the filtered sample (peak 1 in Fig. 5a) were not determined.

Physical characteristics of the intracellular crystals, such as their needle-like crystal habit, provided only limited information on identity, because several compounds crystallize as needles, including 22OHC (Fig. 1c). Even cholesterol monohydrate, whose thermodynamically stable crystalline form is the plate-like form shown in Fig. 1b, does not necessarily nucleate as plates. Rather, it may undergo a series of morphological transformations including needles or filaments (22). The ini-

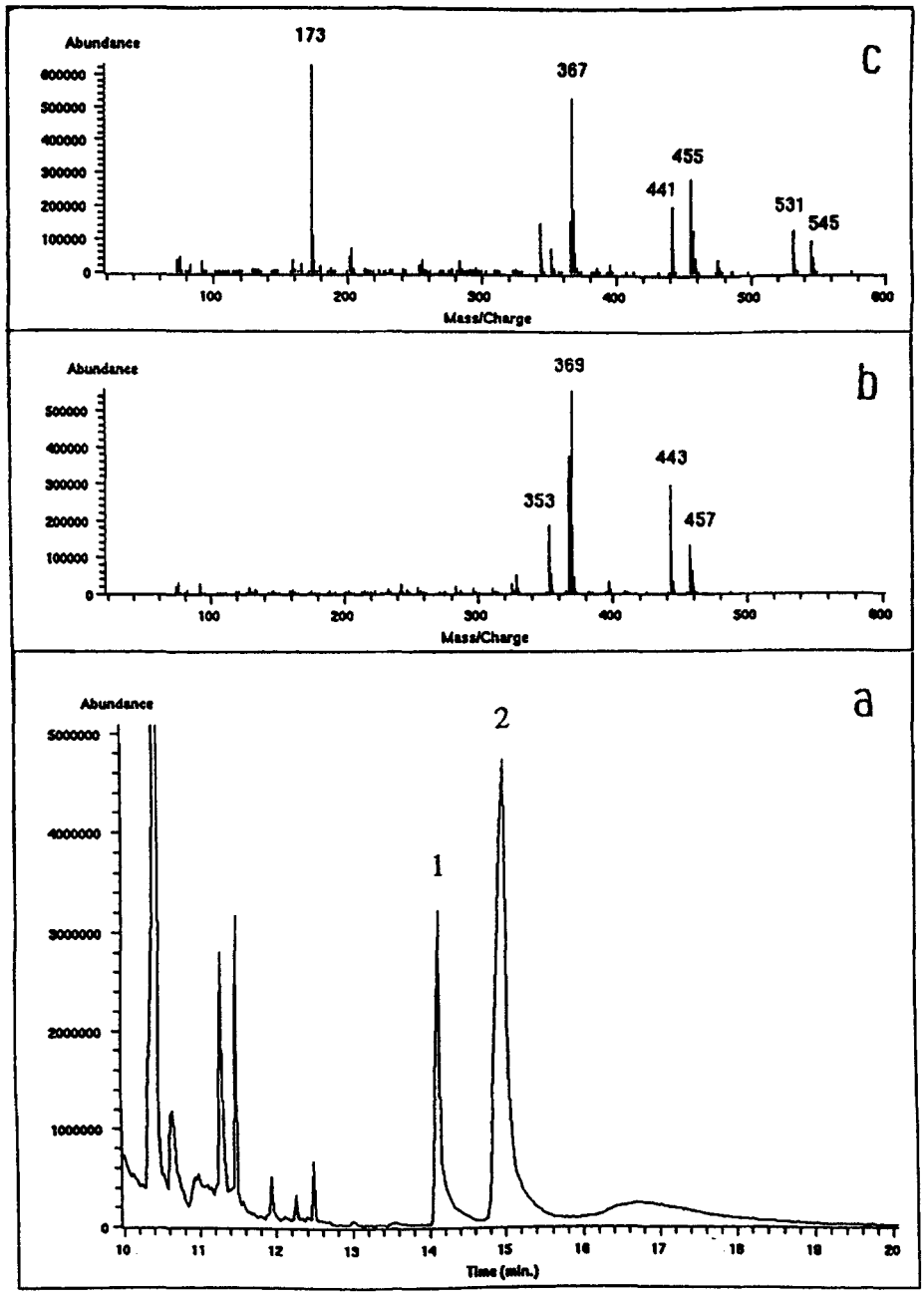

Fig. 5. a) Gas chromatogram of filtered crystals and cellular debris. Peak 1, with a retention time of 14.1 min, corresponds to pure cholesterol, and its PCI mass spectrum is shown in (b). Peak 2, with a retention time of 14.9 min, corresponds to 22OHC, and its PCI mass spectrum is shown in (c). Retention times and PCI mass spectra of peaks 1 and 2 match those of cholesterol and 22OHC standards, respectively.

tial formation of cholesterol needles within cells may therefore serve as a base for 22OHC crystallization. The mechanism of crystallization and its dependence upon cellular activity, however, will require further study, a task for which Raman microspectroscopy is well suited.

This work demonstrates the potential of Raman microspectroscopy in lipid research, especially in the rapid characterization of intracellular crystals. This non-invasive, non-destructive technique achieves high spatial resolution and provides molecular information in situ.

The authors greatly appreciate the instrument loan provided by Instruments, S.A., Inc. We also thank Mrs. Sharon Gong

Rank for preparing the cell cultures and Dr. Howard Schaffer for technical assistance. These studies were supported by grants from the National Heart, Lung, and Blood Institute (HL-51055) and Wisconsin affiliate of the American Heart Association.

Manuscript received 14 November 1996, in revised form 3 March 1997, and in re-revised form 5 May 1997.

REFERENCES

1. Ross, R. 1993. The pathogenesis of atherosclerosis: a perspective for the 1990s. *Nature.* **362:** 801–809.
2. Small, D. M. 1988. Progression and regression of atherosclerotic lesions. *Arteriosclerosis.* **8:** 103–129.
3. Carpenter, K. L. H., S. E. Taylor, C. Van der Veen, B. K. Williamson, J. A. Ballantine, and M. J. Mitchinson. 1995. Lipids and oxidised lipids in human atherosclerotic lesions at different stages of development. *Biochim. Biophys. Acta.* **1256:** 141–150.
4. Breuer, O., S. Dzeletovic, E. Lund, and U. Diczfalusy. 1996. The oxysterols cholest-5-ene-3β,4α-diol, cholest-5-ene-3β,4β-diol and cholestane-3β,5α,6α-triol are formed during in vitro oxidation of low density lipoprotein, and are present in human atherosclerotic plaques. *Biochim. Biophys. Acta.* **1302:** 145–152.
5. Wohlfeil, E. R., and W. B. Campbell. 1997. 25-Hydroxycholesterol enhances eicosanoid production in cultured bovine coronary artery endothelial cells by increasing prostaglandin G/H synthase-2. *Biochim. Biophys. Acta.* **1345:** 109–120.
6. Tangirala, R. K., W. G. Jerome, N. L. Jones, D. M. Small, W. J. Johnson, J. M. Glick, F. H. Mahlberg, and G. H. Rothblat. 1994. Formation of cholesterol monohydrate crystals in macrophage-derived foam cells. *J. Lipid Res.* **35:** 93–104.
7. Mendelsohn, R. 1986. Biomedical applications of Raman scattering. *In* Spectroscopy in the Biomedical Sciences. R. M. Gendreau, editor. CRC Press, Cleveland, OH. 151–173.
8. Keller, S., B. Schrader, A. Hoffmann, W. Schrader, K. Metz, A. Rehlaender, J. Pahnke, M. Ruwe, and W. Budach. 1994. Application of near-infrared Fourier transform Raman spectroscopy in medical research. *J. Raman Spectrosc.* **25:** 663–671.
9. Buiteveld, H., F. F. M. De Mul, J. Mud, and J. Greve. 1984. Identification of inclusions in lung tissue with a Raman microprobe. *Appl. Spectrosc.* **38:** 304–306.
10. Sudlow, K., and A. Woolf. 1991. Identification of renal calculi by their Raman spectra. *Clin. Chim. Acta.* **203:** 387–394.
11. Baraga, J. J., M. S. Feld, and R. P. Rava. 1992. In situ optical histochemistry of human artery using near infrared Fourier transform Raman spectroscopy. *Proc. Natl. Acad. Sci. USA.* **89:** 3473–3477.
12. Centeno, J. A., K. G. Ishak, F. G. Mullick, W. A. Gahl, and T. J. O'Leary. 1994. Infrared microspectroscopy and laser Raman microprobe in the diagnosis of cystinosis. *Appl. Spectrosc.* **48:** 569–572.
13. Schaeberle, M. D., V. F. Kalasinsky, J. L. Luke, E. N. Lewis, I. W. Levin, and P. J. Treado. 1996. Raman chemical imaging: histopathology of inclusions in human breast tissue. *Anal. Chem.* **68:** 1829–1833.
14. Wentrup-Bryne, E., L. Rintoul, J. L. Smith, and P. M. Fredericks. 1995. Comparison of vibrational spectroscopic techniques for the characterization of human gallstones. *Appl. Spectrosc.* **49:** 1028–1036.
15. Duindam, H. J., G. F. J. M. Vrensen, C. Otto, G. J. Puppels, and J. Greve. 1995. New approach to assess the cholesterol distribution in the eye lens: confocal Raman microspectroscopy and filipin cytochemistry. *J. Lipid Res.* **36:** 1139–1146.
16. Le Cacheux, P., G. Menard, H. N. Quang, P. Weinmann, M. Jouan, and N. Q. Dao. 1996. Quantitative analysis of cholesterol and cholesterol ester mixtures using near-infrared fourier transform Raman spectroscopy. *Appl. Spectrosc.* **50:** 1253–1257.
17. Revtyak, G. E., M. J. Hughes, A. R. Johnson, and W. B. Campbell. 1988. Histamine stimulation of prostaglandin and HETE synthesis in human endothelial cells. *Am. J. Physiol.* **225:** C214–C225.
18. Craven, B. M. 1976. Crystal structure of cholesterol monohydrate. *Nature.* **260:** 727–729.
19. Shieh, H. S., L. G. Hoard, and C. E. Nordman. 1977. Crystal structure of anhydrous cholesterol. *Nature.* **267:** 287–289.
20. Garti, N., L. Karpuj, and S. Sarig. 1981. Correlation between crystal habit and the composition of solvated and nonsolvated cholesterol crystals. *J. Lipid Res.* **22:** 785–791.
21. Faiman, R. 1977. Raman spectroscopic studies of different forms of cholesterol and its derivatives in the crystalline state. *Chem. Phys. Lipids.* **18:** 84–104.
22. Konikoff, F. M., D. S. Chung, J. M. Donovan, D. M. Small, and M. C. Carey. 1992. Filamentous, helical, and tubular microstructures during cholesterol crystallization from bile. *J. Clin. Invest.* **90:** 1155–1160.